SATELLITE-DETECTED ANOMALOUS CHANGES IN PARAMETERS OF VARIOUS GEOPHYSICAL FIELDS DURING EARTHQUAKES OF $6 \leq M \leq 7.8$ IN TÜRKIYE IN FEBRUARY 2023

V. G. Bondur[1],[*] ⓘ, M. N. Tsidilina[1] ⓘ, E. V. Gaponova[1] ⓘ, O. S. Voronova[1] ⓘ, M. V. Gaponova[1] ⓘ, N. V. Feoktistova[1] ⓘ, and A. L. Zima[1] ⓘ

[1]Institute for Scientific Research of Aerospace Monitoring "AEROCOSMOS", Moscow, Russia

[*] **Correspondence to:** Valery G. Bondur, office@aerocosmos.info

Abstract: Research was conducted using satellite data to study variations in parameters of various geophysical fields manifested in the lithosphere, atmosphere, and ionosphere during the preparation and occurrence of destructive earthquakes of $6 \leq M \leq 7.8$ in Türkiye in February 2023. Precursor manifestations of these seismic events were satellite-detected in the form of anomalies in parameters of various geophysical fields, including: lineament systems, surface skin temperature and surface air temperature, relative humidity, latent heat flux, integrated flux of outgoing longwave radiation, altitude changes in ionospheric electron density, total electron content of the ionosphere, as well as aerosol optical depth. It was found that the anomalies of all studied geophysical fields detected using satellite data manifested most intensively during the period 3–13 days before the onset of seismic events.

Citation: Bondur, V. G., M. N. Tsidilina, E. V. Gaponova, O. S. Voronova, M. V. Gaponova, N. V. Feoktistova, and A. L. Zima (2024), Satellite-Detected Anomalous Changes in Parameters of Various Geophysical Fields During Earthquakes of $6 \leq M \leq 7.8$ in Türkiye in February 2023, *Russian Journal of Earth Sciences*, 24, ES4006, EDN: BRWHCY, https://doi.org/10.2205/2024es000930

1. Introduction

Earthquakes are among the most destructive and least predictable natural disasters. Vast territories, often densely populated, are under the threat of earthquakes. Some of these natural disasters were devastating earthquakes that occurred in Türkiye and neighboring countries in February 2023.

Over the past 23 years (from 2000 to 2023), more than 7000 earthquakes of $5 \leq M \leq 7.8$ have occurred in Türkiye, including 240 seismic events of $5 \leq M \leq 6$ and around 20 events of $M \geq 6$ [*Federal Research Center Geophysical Survey of the RAS*, 2023; *United States Geological Survey*, 2023]. The destructive seismic events that occurred in February 2023 in southeastern Türkiye and Syria, including the catastrophic $M7.8$ earthquake on 6 February 2023, once again vividly demonstrated how massive and devastating their effects can be [*Akhoondzadeh and Marchetti*, 2023; *Bondur et al.*, 2023; *Dal Zilio and Ampuero*, 2023; *Ruzhich et al.*, 2023]. According to the Turkish government, these earthquakes resulted in the death of over 50 thousand people, injuries to over 107 thousand people, and economic losses exceeding 103 billion US dollars. In order to forecast such dangerous natural disasters as earthquakes, it is important to register their precursors [*Sobolev and Ponomarev*, 2003]. The search for earthquake precursors is a quite challenging task [*Keilis-Borok et al.*, 2009; *Mogi*, 1985; *Molchan and Keilis-Borok*, 2008; *Sobolev and Ponomarev*, 2003].

Methods and tools of satellite monitoring play a crucial role in addressing this task [*Akhoondzadeh and Marchetti*, 2023; *Bondur and Smirnov*, 2005; *Bondur et al.*, 2022, 2023; *Mikhailov et al.*, 2023a,b; *Xu et al.*, 2022; *Zhang et al.*, 2021]. The current level of their development and the data products obtained through satellite monitoring allow for the

study of anomalous variations in parameters of various geophysical fields during the preparation and occurrence of significant seismic events [*Bondur et al.*, 2022]. Satellite data can be used to register changes in lineament systems, which help to identify structural deformations in epicentral zones and the kinematics of active faults before earthquakes [*Bondur et al.*, 2022]. Anomalies occurring at different heights before an earthquake can also be detected by studying thermal fields from the Earth's surface to the upper cloud boundary [*Bondur et al.*, 2022; *Pulinets et al.*, 2006; *Tronin*, 2000; *Xiong et al.*, 2010]. Anomalies in various ionospheric parameters during the preparation and occurrence of seismic events can be recorded by satellite navigation systems [*Bondur and Smirnov*, 2005; *Bondur et al.*, 2022; *Pulinets and Ouzounov*, 2011; *Smirnov and Smirnova*, 2008]. To register anomalous geodynamics before earthquakes, it is promising to use satellite radio interferometry methods [*Bondur et al.*, 2023; *Mikhailov et al.*, 2023a,b; *Xu et al.*, 2022; *Zhang et al.*, 2021] which were used, among others, to analyze the studied earthquake in Türkiye [*Bondur et al.*, 2023; *Mikhailov et al.*, 2023a,b], as well as modeling methods [*Bondur et al.*, 2016; *Soloviev and Gorshkov*, 2017]. Interesting approaches to determining potential locations of strong earthquakes include use of pattern recognition methods presented in a study [*Gvishiani et al.*, 2020].

For a better understanding of the processes related to the preparation and occurrence of strong earthquakes, it is promising to conduct a joint analysis of parameters of various geophysical fields recorded using satellites during the monitoring of seismically hazardous areas [*Bondur et al.*, 2022; *Jiao et al.*, 2018; *Pulinets and Ouzounov*, 2011].

In this study, a joint analysis of anomalous variations in geophysical fields manifested in the lithosphere, atmosphere, and ionosphere during preparation and occurrence of destructive Türkiye earthquakes in February 2023 was carried out.

2. Research methodology

In order to identify changes in significant parameters of various geophysical fields during the preparation and occurrence of destructive earthquakes in Türkiye in February 2023, an analysis was conducted for changes in lineament systems, parameters of thermal fields and relative humidity, aerosol optical depth (AOD), as well as altitude distribution in ionospheric electron density (N_e) and ionospheric total electron content (TEC).

The assessment of the location of lineament systems was carried out through automated analysis of satellite image fragments of 100×100 km obtained from the Terra satellite (MODIS instrument) with a spatial resolution of 250 meters. Based on the results of this analysis, statistical characteristics of local lineaments (stripes) and rose diagrams of regional lineaments were constructed. For each stripe, the orientation was determined for eight directions: 0°, 22.5°, 45°, 67.5°, 90°, 112.5°, 135°, 157.5° (angle was measured from right to left horizontally) [*Bondur et al.*, 2022].

The total lengths of lineaments (L) were calculated for eight directions using the formula (1):

$$L = \frac{nr}{1000 \cos \varphi}, \tag{1}$$

where n is the number of pixels; r is the spatial resolution; and φ is the angle of lineament orientation.

As a result, graphs of relative changes in the total lengths of stripes in different directions were constructed and analyzed.

Studies for the seismic activity period in Türkiye were conducted using such parameters of thermal fields as Surface Skin Temperature (SST), Surface Air Temperature (SAT), Latent Heat Flux (LHF) and Outgoing Longwave Radiation (OLR) as well as a parameter of Relative Humidity at Surface (RHS).

Parameters SST, SAT, RHS, and OLR were registered by the AIRS instrument (Aqua satellite) [*Hearty et al.*, 2013]. LHF data with 6-hour averaging were obtained from the reanalysis dataset available on the Google Earth Engine cloud platform [*Saha et al.*, 2010].

In the study of thermal fields and RHS, a methodology based on the use of the standard deviation interval ($\mu \pm \sigma$) relative to the mean values (μ) was applied. The study area for parameters (SST, SAT, RHS, LHF, OLR) was the zone with coordinates 35°N–40°N, 35°E–40°E including the territory where epicenters of earthquakes were located.

The research of the studied parameters was conducted for the period from January to March 2023, as well as for multi-year data for these months (from 2004 to 2022). A specially developed software module was used for the joint analysis of these parameters [*Bondur et al.*, 2022]. The resulting values were transformed into numerical features within the range of 0 to 1 using formula (2):

$$N_i = \frac{1}{1 + \exp\left(-\left(\frac{(S_d - S^*)}{\sigma}\right)\right)},\tag{2}$$

where S_d – data for the current day; S^* – arithmetic mean of previous years; σ – standard deviation.

In studying the dynamics of aerosols in the atmosphere during the preparation and occurrence of the analyzed earthquakes, the AOD parameter for the green band of the electromagnetic spectrum (0.55 µm) was used. This parameter was contained in the MCD19A2 Level 2 data product, which combines data from the Terra and Aqua satellites [*Lyapustin and Wang*, 2018]. The data acquisition and processing to detect changes in AOD in the study area were done using the Google Earth Engine platform for scientific analysis and visualization of geospatial data [*Google Earth Engine*, 2023]. Daily average AOD values over land for the study area in Türkiye were obtained based on MCD19A2. Values calculated from satellite image fragments containing less than 1000 pixels were discarded as unreliable data.

For analyzing AOD anomalies, a zone of approximately 140×220 km around the earthquake epicenter was used. This size of the study area was chosen to exclude the influence of other aerosol sources such as, for example, UV-absorbing dust particles from the Arabian Peninsula (Syrian Desert).

The variations in ionospheric plasma parameters were studied based on analysis of GPS data using two approaches. The analysis of altitude changes in N_e was conducted using a methodology based on radio occultation of Earth's ionosphere, measuring radio signal parameters obtained from existing satellite navigation systems. This method involves solving inverse problems of radio wave refraction, which are inherently unstable and require special mathematical methods to consider additional information about the active task [*Bondur and Smirnov*, 2005; *Smirnov and Smirnova*, 2008].

The method allows for registering altitude distribution of N_e in quasi-real-time mode based on data from a single ground station, which is particularly important for remote and inaccessible regions of the Earth [*Bondur and Smirnov*, 2005].

As a result of navigation data processing, altitude profiles of N_e were obtained along trajectories of subionospheric points for altitudes ranging from 80 to 1000 km with a 30-second discreetness based on HRMN site data.

To conduct a joint analysis of ionospheric plasma parameter variations with characteristics of other geophysical fields based on long-term data, a normalized index of total electron content of the ionosphere (NTEC) was calculated using formula (3):

$$\text{NTEC} = \frac{(\text{TEC} - \mu)}{\sigma},\tag{3}$$

where TEC represents the values of total electron content for the current day in 2023 obtained from Global Ionospheric Maps (GIM) [*Noll*, 2010] for the zone with coordinates 35°N–40°N, 35°E–40°E; μ is the arithmetic mean of past years (2001–2022) for the studied day; σ is the standard deviation.

In the final stage of the research, a joint analysis of anomalous variations in lineament systems, thermal fields, RHS, AOD, and ionospheric parameters was conducted to identify correlations between the characteristics of various geophysical fields.

3. Research results and their analysis

3.1. Aspects of seismic activity in the studied region

The strongest earthquakes ($M \geq 6$) in the study area are associated with the deep East Anatolian and North Anatolian faults [*Trifonov*, 2017].

In the first three months of 2023, about 500 earthquakes of $M \geq 3.4$ occurred in the East Anatolian fault zone. Figure 1 shows the locations of earthquake epicenters in Türkiye with $M \geq 4$ (a), as well as a graph of earthquake magnitudes in the East Anatolian fault zone during the first three months of 2023 (b) according to [*Federal Research Center Geophysical Survey of the RAS*, 2023; *United States Geological Survey*, 2023].
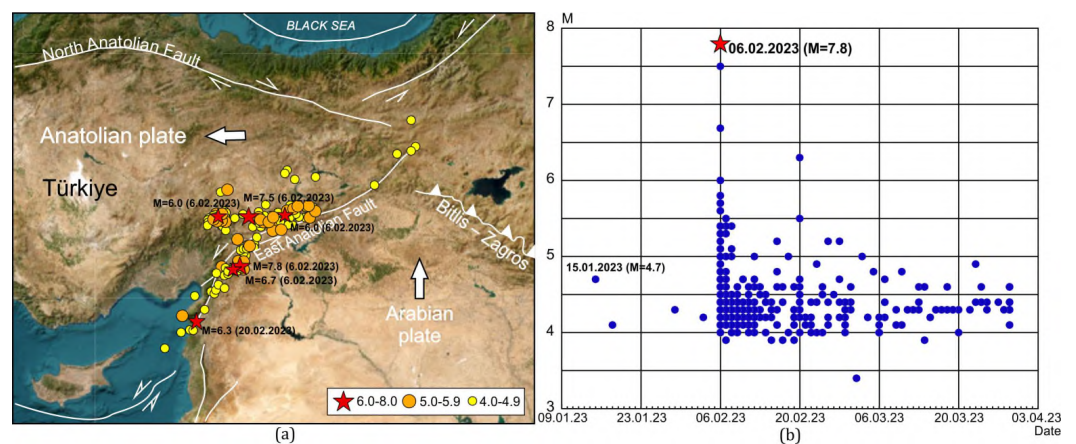

Figure 1. Earthquake epicenter locations in Türkiye (a) and graph of earthquake magnitudes in the East Anatolian fault zone during the first three months of 2023 (b) according to [*United States Geological Survey*, 2023].

Starting from 6 February 2023, five destructive earthquakes of $5 \leq M \leq 7.8$ occurred in Türkiye, along with approximately 200 aftershocks of $4 \leq M \leq 6$. The epicenter of the strongest $M = 7.8$ earthquake was located 27 km from the city of Gaziantep. The focal depth was 17.9 km [*United States Geological Survey*, 2023].

3.2. Results of the analysis of lineament systems

Lineaments were constructed for the epicentral area based on fragments of satellite images in Figure 2. The earthquake epicenter fell within the upper right corners of the satellite image fragments.

Analysis of rose diagrams of regional lineaments in Figure 2 showed that changes in intersecting lineaments (oriented at 315° relative to the main relief structures) occurred before the seismic events under study. This effect is supported by the findings of [*Bondur et al.*, 2022]. The analysis of Figure 2 indicates that from the beginning of observations (20 November 2022) until 10 January 2023, the predominant directions of lineaments of rose diagrams (45°) and their intersecting directions (315°) changed slightly. From 23 to 25 January 2023, there was a decrease in the rays of rose diagrams with directions of 45°, while the rays oriented NW–SE (315°) increased, reaching their maximum length on 3 February 2023 (3 days before the earthquake). They became approximately equal in length to the rays of rose diagrams with directions of 45°.

On the diagrams of elongation lines of local lineaments (stripes) in Figure 2, it can be observed that from 19 December 2022 to 10 January 2023 (5–27 days before the $M = 4.7$ foreshock), there was an increase in elongation lines of stripes in the NE–SW direction (45°). Starting from 23 January 2023 (14 days before the earthquake $M = 7.8$), they gradually changed their orientation towards sub-latitudinal directions (as indicated by red arrows in
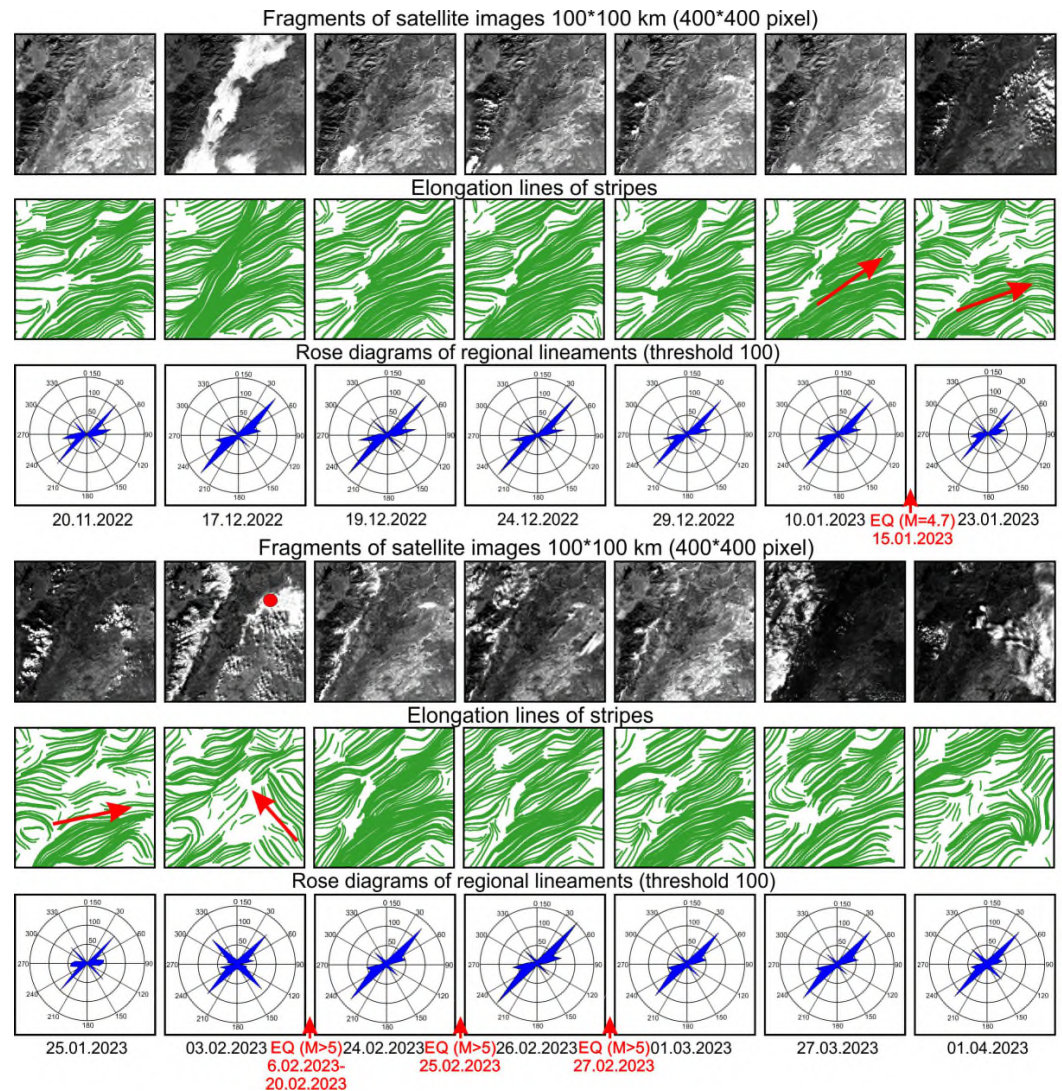
Figure 2. Fragments of satellite images, elongation lines of stripes, and rose diagrams of regional lineaments before the earthquakes on 6 February 2023.

Figure 2). Additionally, on the diagram of elongation lines of stripes obtained on 3 February 2023 (3 days before the earthquake $M = 7.8$), an increase in their quantity was detected for NW–SE directions (315°), intersecting with the main relief structures.

3.3. Results of the analysis of thermal fields and relative humidity

Figure 3 presents graphs of changes of SST, SAT, RHS, LHF, and OLR from 1 January to 1 March 2023, compared to the long-term values for these months from previous years (2004–2022). Values of the parameters were considered anomalous if they exceeded the quadratic mean range ($\pm\sigma$).

Analysis of the results presented in Figure 3 showed that the variations of background values (2011 year) of the selected parameters of thermal fields and RHS were moderate and practically did not exceed the intervals of standard deviations.

As a result of the analysis of the changes in the studied parameters (Figure 3), anomalies were identified before the foreshock on 15 January 2023 ($M = 4.7$), as well as before the main earthquake on 6 February 2023 ($M = 7.8$), which are described below.

An anomalous downward trend in SST and SAT changes by 7–8 °C was observed from 2 January 2023, while RHS values rose by 24%. Similar opposite trends in temperature and humidity were studied during several earthquakes in Mexico, for example, in the work

of [*Pulinets et al.*, 2006], where the possibility of using these parameters as indicators of impending seismic activity was confirmed.

Since 3 January 2023, anomalous changes in the studied parameters were detected, which manifested in the form of a decrease in temperature and an increase in humidity. After the increase in RHS values, there was a LHF rise starting from 5 January 2023 (by $13\,\mathrm{W/m^2}$).

Anomalous OLR changes were detected during the period from 1 to 12 January 2023, when there was a decrease in values of this parameter by $72\,\mathrm{W/m^2}$.

On 6 February 2023, abnormal changes of the studied parameters were identified (Figure 3). Starting from 14 January 2023, there was an increase in SST and SAT by 5–9 °C above the epicentral area of the impending earthquake. It facilitated intense interaction between land and atmosphere, followed by an LHF increase (by $28\,\mathrm{W/m^2}$). The LHF is strongly influenced by meteorological parameters such as RHS. The increase (up to 86%) in RHS values detected since 12 January 2023 probably caused an increase in the amount of water vapor in the atmosphere (Figure 3). Water vapor carries latent heat, which is released or absorbed during phase changes of water in the process of evaporation or condensation [*Cervone et al.*, 2005]. Therefore, the elevated RHS values from 15 January to 2 February 2023, compared to long-term averages, could have contributed to the LHF increase. The maximum of this parameter ($40.5\,\mathrm{W/m^2}$) was revealed on 2 February 2023, four days before the main earthquake (Figure 3). The maximum LHF increase before an earthquake and the strengthening of its interaction between the atmosphere and land are described in the works [*Dey and Singh*, 2003; *Tronin*, 2000].

Analysis of Figure 3 showed that during the preparation period for the main seismic event (6 February 2023), starting from 19 January 2023 abnormally high OLR values were recorded using satellite data. Their maximum value was $252\,\mathrm{W/m^2}$ on 21 January 2023. Next, from 21 January to 4 February 2023, there was a gradual decrease in OLR values by $96\,\mathrm{W/m^2}$.

Besides the decrease in OLR values, a decrease in SST and SAT values by 11–14 °C was observed from 19 January to 2 February 2023 (Figure 3). SST changes prior to destructive earthquakes in Türkiye on 6 February 2023 were also described in the work [*Akhoondzadeh and Marchetti*, 2023], where a decrease by 5–8 °C approximately 18 days before the main seismic event was demonstrated.

3.4. Analysis of aerosol optical depth anomalies

In a number of studies, for example, [*Akhoondzadeh*, 2015; *Bondur et al.*, 2022; *Ganguly*, 2016; *Ghosh et al.*, 2023; *Okada et al.*, 2004] a relation was discovered between AOD anomalies (including those identified using satellite data) and strong earthquakes.

In this work we studied AOD changes based on satellite data during the preparation and occurrence of destructive earthquakes in Türkiye in February 2023.

Figure 4a,b show maps of the study areas with fault lines and epicenters of the main earthquakes that occurred in 2023 (a) and 2020 (b) as well as graphs of AOD changes. Figure 4c shows the average daily AOD values in January–February 2023. The Figure also presents comparison of the daily average AOD values for the previous 10 years and the average daily values for the background year 2011 for the same period.

Analysis of Figure 4c showed that during the period of preparation and occurrence of earthquakes from 15 January to 1 March 2023, low AOD values were observed relative to the average annual value for the previous 2022. The exceptions were AOD values recorded on 15 January, 28 January and 27 February 2023. These days, daily average AOD values exceeded the limit of three standard deviations (3σ) from the annual mean (yellow background). On 15 January 2023, a $M4.7$ earthquake was recorded. It should be noted that some of the data is missing due to cloudiness over the studied region.

Figure 4c shows that from 21 to 28 January 2023 the AOD value continuously increased and reached a maximum value (0.39) on 28 January 2023 (7 days before the earthquake $M = 7.8$), significantly exceeding the 99% confidence interval ($\mu + 3\sigma$). Next, from 29 Jan-
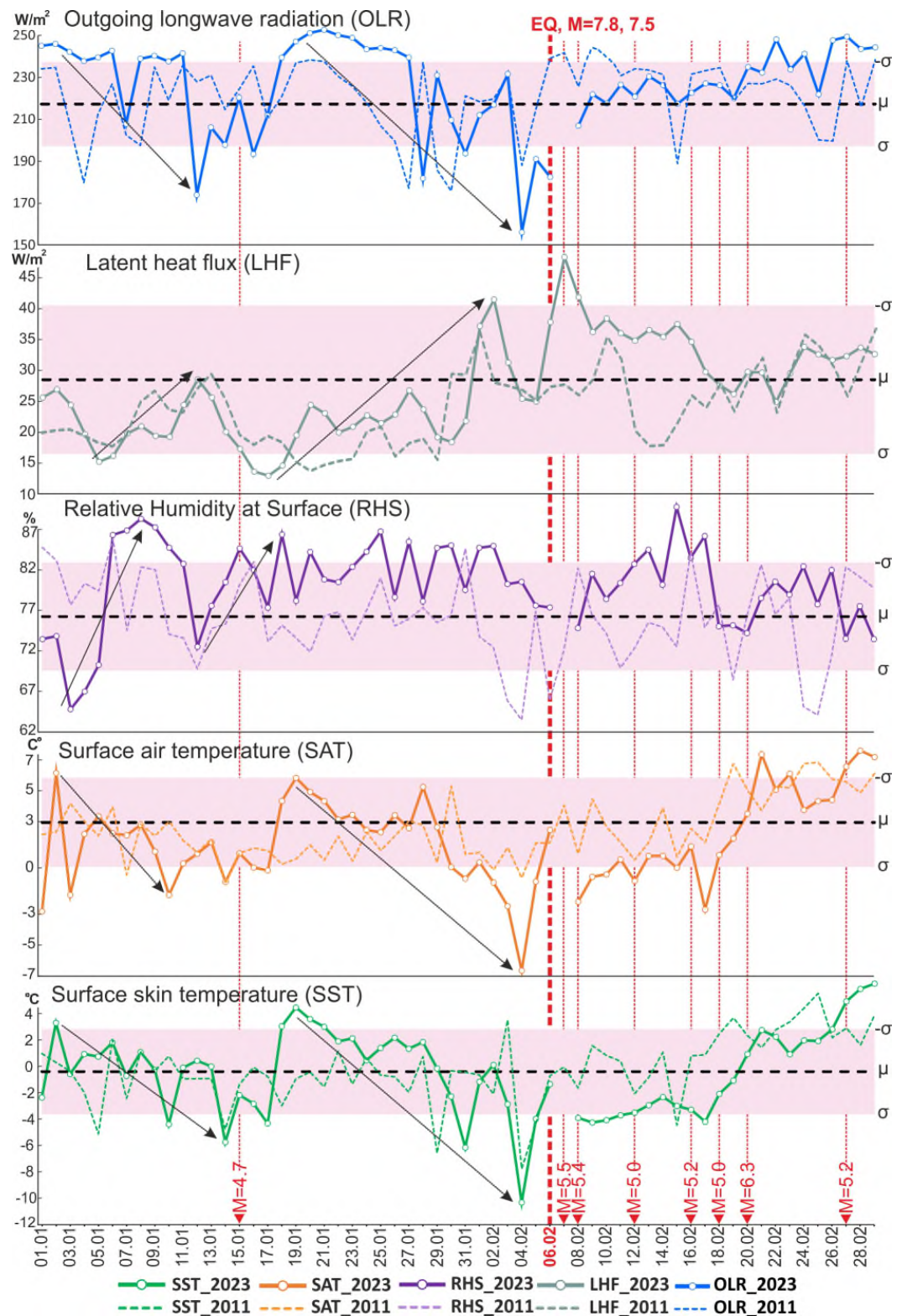
Figure 3. Variations in the values of SST and SAT, RHS, LHF, and OLR during the preparation and occurrence of earthquakes in Türkiye from 1 January to 1 March 2023.

uary to 2 February 2023, there was a decrease of AOD values and a slight increase (up to 0.24) on 4 February 2023 (2 days before the earthquake $M = 7.8$). In the period from 7 to 17 February decreased AOD values were observed. Then, on 20 and 27 February 2023 high

AOD values were identified, reaching 0.24 and 0.309 on the days of aftershocks of $M = 6.3$ and $M = 5.2$, respectively (Figure 4c).

During the study, AOD variations were also researched for other earthquakes that occurred in the zone of the East Anatolian Fault. Similar AOD anomalies detected 4–7 days before the earthquakes were identified in the area where earthquake series occurred in 2020 (Figure 4b): on 4 August four earthquakes with $4 \leq M \leq 5.6$ were recorded, and on 8 September – three earthquakes with $4.2 \leq M \leq 4.7$. Analysis of Figure 4d shows a gradual increase in AOD values from 19 to 28 July 2020, reaching a peak value of 0.46 detected 7 days before the earthquakes on 4 August 2020. This was followed by a sharp decrease in AOD values below the average annual value.

The anomaly in AOD values detected on 2 September 2020, before the second series of earthquakes, is weaker and does not exceed the level $(\mu + 3\sigma)$, the increase in AOD values was observed for only 4 days reaching a value of 0.34 (Figure 4d).

Thus, based on the results of the analysis of the graphs shown in Figure 4c,d, possible precursor AOD anomalies include a smooth increase in values of this parameter and are going beyond the 99% confidence interval, followed by a decline 6–7 days before significant seismic events. For a more detailed analysis of anomalous AOD changes before seismic events, it is planned to obtain additional data.

3.5. Analysis of ionospheric plasma anomalies

In order to identify anomalous variations of ionospheric parameters during earthquake preparation and occurrence, altitude changes in N_e.

N_e changes in the epicentral region from 24 January to 13 February 2023 were studied based on data Satellites 12 and 24 from the HRMN site (Figure 5a). The satellites' pass times over the study area were as follows: satellite 12: 13:00–20:00 LT; satellite 24: 13:00–18:00 LT.

Figure 5b and 5c show the time series of altitude profile changes in N_e obtained from satellites 12 and 24 in the epicentral zone before the earthquakes in Türkiye in 6 February 2023.

From the analysis of Figure 5b, it follows that from 24 to 28 January 2023, the N_e values remained almost unchanged according to data from satellite 12. Starting from 29 January 2023, there was a gradual decrease. The minimum N_e was recorded on 3 February 2023, three days before the earthquakes of $M = 7.8$ and $M = 7.5$ that occurred on 6 February 2023. The decrease in N_e values amounted to ~ 30% compared to the values registered during the period from 24 to 28 January 2023. A sharp N_e increase was observed on the day of the earthquake on 6 February 2023, which amounted to ~ 42% compared to the previous day.

The analysis of changes in altitude profiles of N_e based on data from satellite 24 (Figure 5c) is identical to the changes registered by satellite 12 (Figure 5b), namely, a N_e drop from 29 January to 3 February 2023 by ~ 20% and a sharp increase by ~ 30% on the day of the earthquakes of $M = 7.8$ and $M = 7.5$ on 6 February 2023 (Figure 5c).

The period from 1 to 10 January 2023 was considered to study background N_e values in the same region (Figure 5d). From the analysis of Figure 5d, it follows that no significant changes in N_e were observed during this period. No earthquakes were recorded during this period, and the geomagnetic conditions were relatively calm, except for 4 January 2023, when a moderate disturbance in the geomagnetic field was observed ($Dst = -61$ nT) [World Data System, 2023].

Thus, the analysis of altitude profiles of the N_e revealed anomalous changes, which are expressed in a 20–30% drop in the N_e values on 3 February 2023 (3 days before the earthquake) and in a sharp increase by 30–42% on 6 February 2023 (the first day of the earthquake series) (Figure 5b, c).

The decrease in ionospheric parameter values identified in our study, which occurred 3 days before the start of the earthquake series in Türkiye, coincides with the results
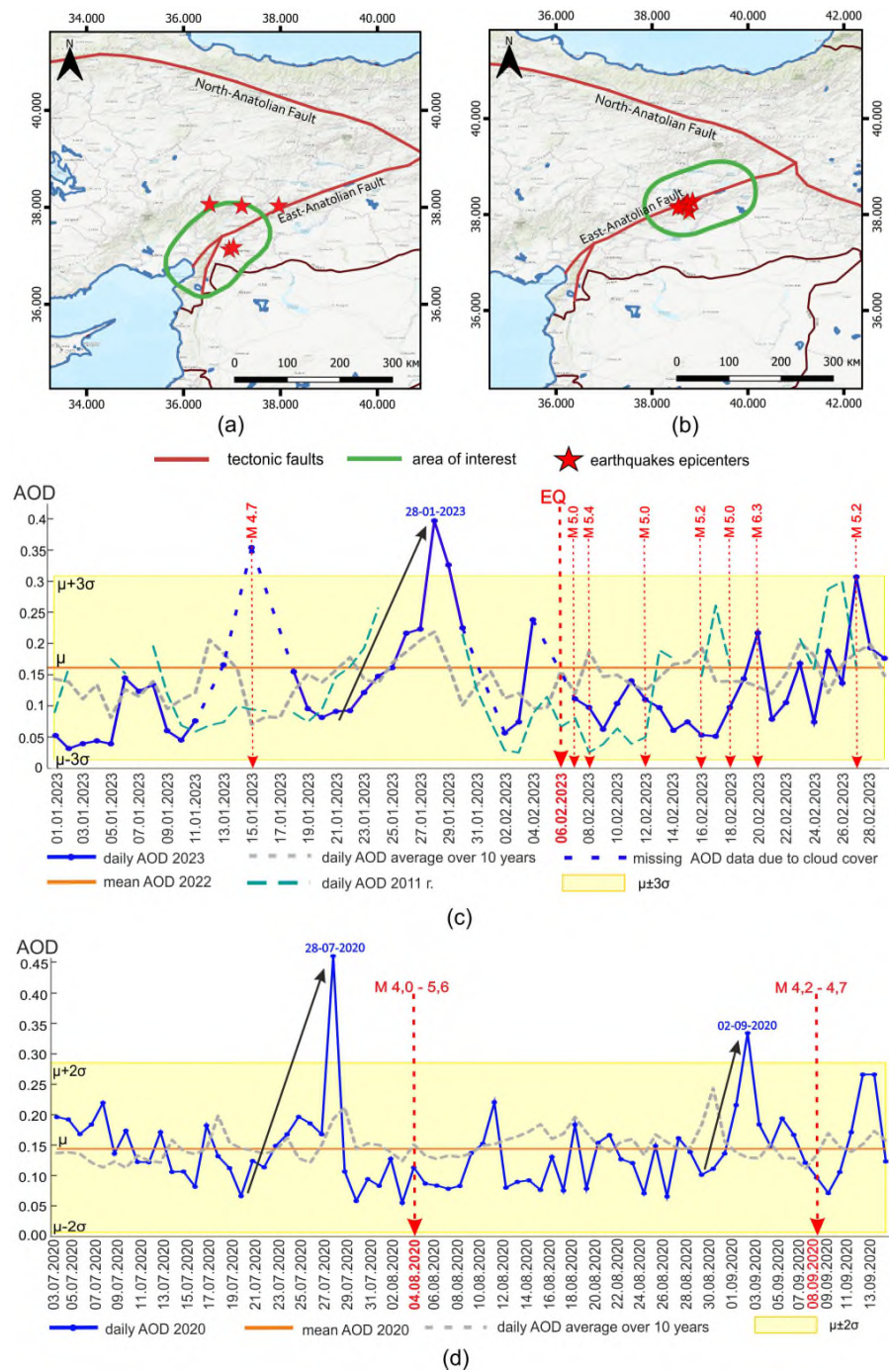
Figure 4. Study areas of AOD for earthquakes that occurred in 2023 (a) and 2020 (b); changes in average daily AOD values during the preparation of earthquakes that occurred in Türkiye on 6 February 2023 (c) and in August-September 2020 (d).

of ionospheric research for this earthquake described in the work by [*Akhoondzadeh and Marchetti*, 2023].

These anomalies can be used as ionospheric precursors of significant seismic events, which can be recorded based on satellite data.

3.6. Joint analysis of anomalies in various geophysical fields

A joint analysis was conducted to identify correlations between the occurrence of anomalous changes in parameters of various geophysical fields during preparation of earthquakes in Türkiye in February 2023.
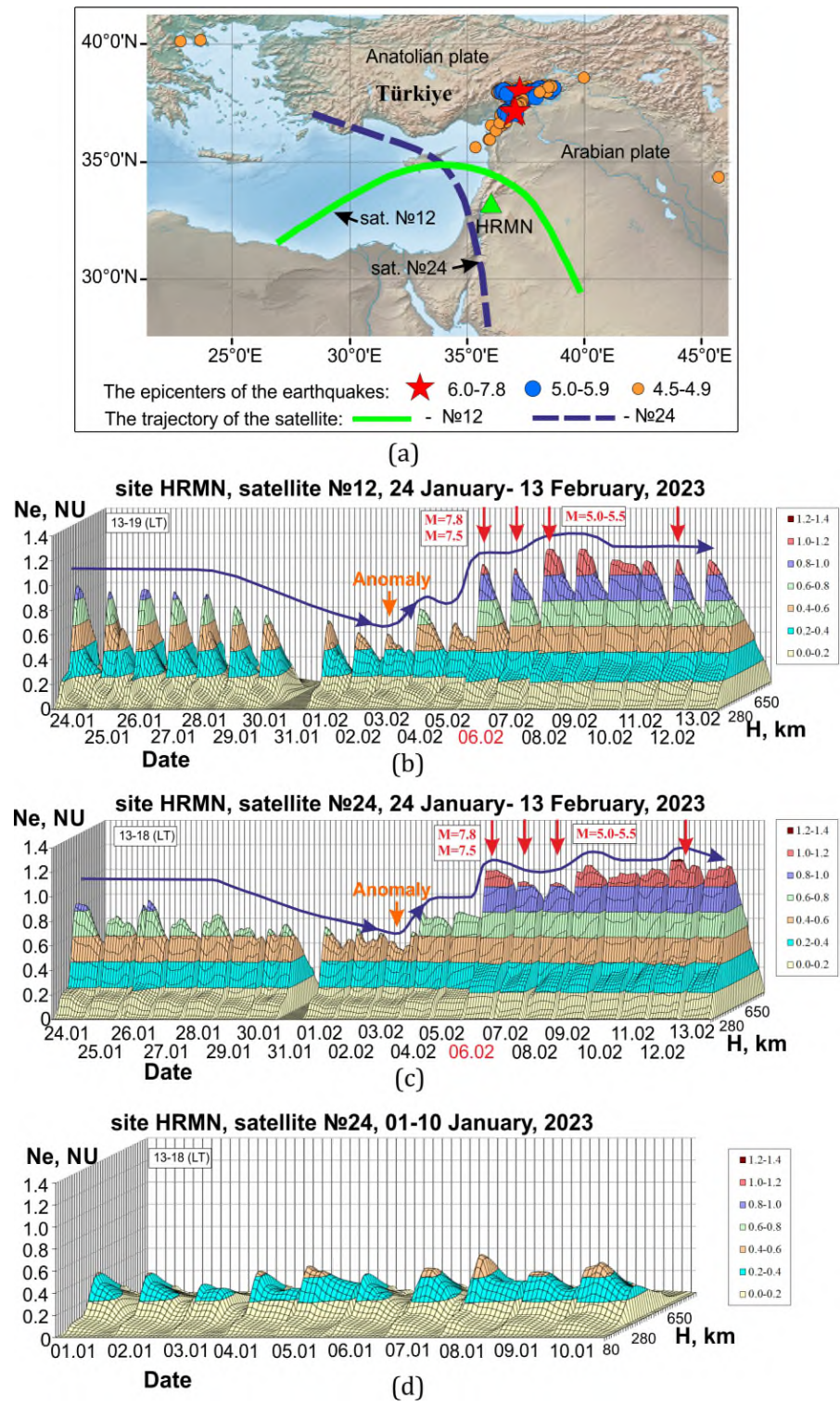
Figure 5. Map of HRMN site location and trajectories of sub-ionospheric points of Satellites 12 and 24 (a); altitude profiles of N_e during the period from 24 January to 13 February 2023, obtained from satellites 12 (b) and 24 (c); from 1 to 10 January 2023, obtained from satellite 24 (d) for HRMN site.

Figure 6 shows graphs of changes in the normalized index of total electron content of the ionosphere (NTEC), calculated using formula (3), normalized index of outgoing longwave radiation (N_{OLR}), normalized index of latent heat flux (N_{LHF}), normalized index of relative humidity (N_{RHS}), normalized index of surface air temperature (N_{SAT}), and normalized index of surface skin temperature (N_{SST}), calculated using formula (2), daily

average values of AOD, as well as graphs of changes in total lengths of lineaments of various directions for the period from 1 January to 28 February 2023.

From the analysis of Figure 6, it follows that before the series of destructive earthquakes that occurred in Türkiye in February 2023, anomalies in the atmosphere were registered. These anomalies manifested as a 13% decrease (3 January 2023) and a 55% increase (8 January 2023) in N_{RHS}. The increase in relative humidity contributed to a 22% increase in N_{LHF} occurred from 9 to 12 January 2023. These processes preceded the OLR anomalies, which occurred on 12 January 2023 (25 days prior) and were characterized by a sharp decrease in N_{OLR} values by 54%.

Since a $M = 4.7$ foreshock occurred on 15 January 2023 on the studied territory, the anomalies manifested in the changes of relative humidity, N_{OLR}, and characteristics of lineament systems registered from 3 to 12 January 2023 may be related to this earthquake.

Starting from 18 January 2023 (19 days before the $M = 7.8$ earthquake), anomalies in the characteristics of all studied geophysical fields (Figure 6) were registered, which activated a chain of processes preceding the series of strong earthquakes that occurred in Türkiye in February 2023.

Analysis of Figure 6 showed that from 23 January 2023 (14 days before the $M = 7.8$ earthquake that occurred on 6 February 2023), a restructuring of the relative values of lineament lengths began. An anomalous N_{RHS} increase by 24% was registered on 25 and 27 January 2023, and a sharp N_{OLR} decrease by 61% was recorded on 28 January 2023. Additionally, an AOD anomaly was registered on 28 January 2023, manifesting as a sharp increase in this parameter by 146% (Figure 4c, Figure 6). Subsequently, on 29 January 2023, N_{OLR} increased by 40%, followed by a decrease of 43% until 4 February 2023.

From 31 January to 3 February, the following changes of the parameters were recorded: a decrease of 22% in NTEC, anomalous increase in N_{LHF} by 35% and N_{RHS} by 28%, anomalous decrease in N_{SAT} by 18% and N_{SST} by 8%. On 3 February 2023 (3 days before the earthquakes that occurred on 6 February 2023), the most significant anomalous changes in relative values of lineament lengths of various directions were identified, characterized by their maximum growth or decline (Figure 6).

Thus, the joint analysis of qualitative changes in lineament systems, anomalies in SST, SAT, RHS, LHF, OLR, AOD, and TEC allowed for the identification of a possible sequence of precursor anomalies in the parameters of the studied geophysical fields during the preparation of a series of destructive earthquakes that occurred in Türkiye in February 2023.

4. Conclusion

Variations in significant parameters of various geophysical fields manifested in the lithosphere, atmosphere, and ionosphere during the preparation and occurrence of destructive earthquakes in Türkiye in February 2023 have been studied using satellite data.

Spatial-temporal variations in lineament systems were identified 14 days before the catastrophic earthquake on 6 February 2023. Anomalous changes in regional lineament systems were registered 3 days before the earthquake on 6 February 2023. They manifested in a significant increase in the rays of rose diagrams of intersecting directions in relation to the directions of the main relief structures (lineaments in the direction of 315° almost doubled).

The analysis of changes in SST, SAT, RHS, LHF, and OLR over epicentral areas of seismic events revealed their similar anomalous behavior before the foreshock on 15 January 2023 ($M = 4.7$) and the catastrophic seismic event on 6 February 2023.

During the preparation of strong earthquakes that occurred in Türkiye in February 2023, a trend towards anomalous decrease of SST and SAT (by 11–14 °C) 18 days before seismic events was identified. Considering the LHF dependence on meteorological parameters such as RHS, the observed RHS increase (up to 86%) 19 days before earthquakes likely contributed to the LHF increase by 26 W/m^2 with its maximum value recorded 4 days
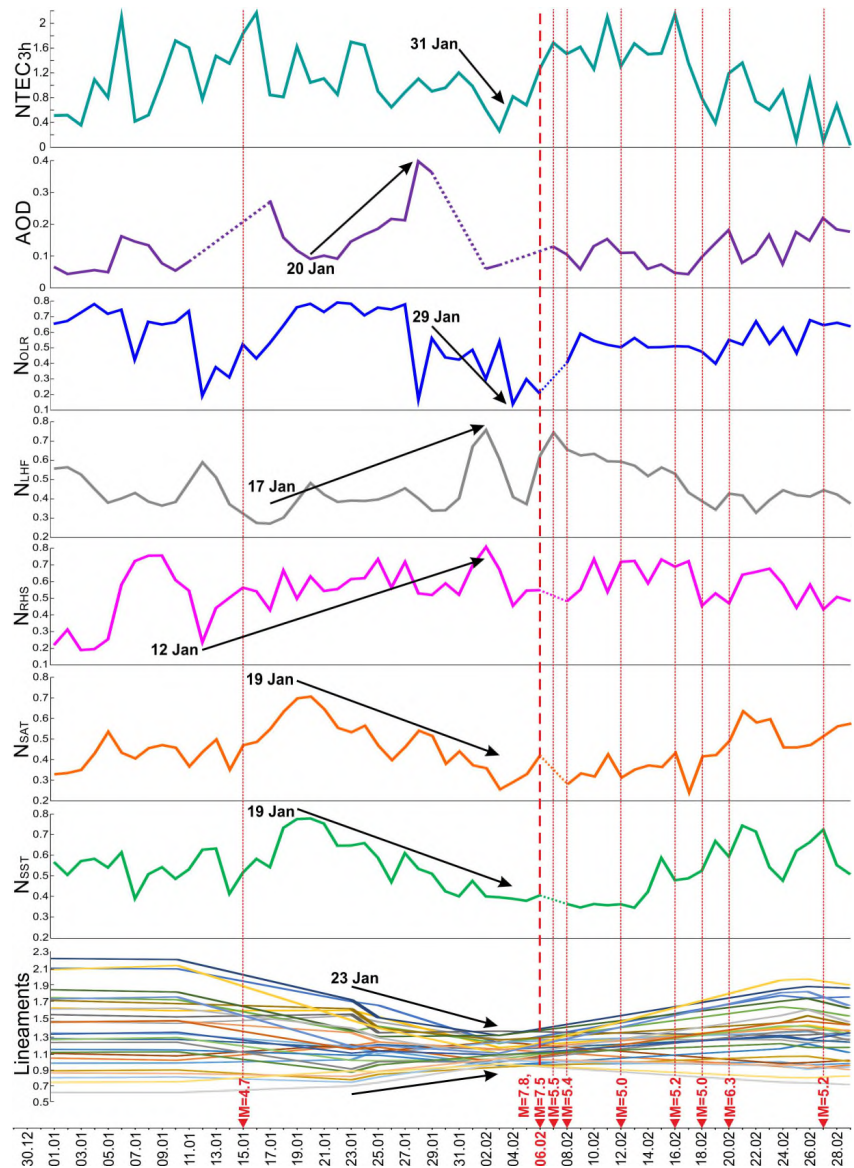
Figure 6. Graphs of changes: NTEC; AOD; N_{OLR}, N_{LHF}, N_{RHS}, N_{SAT} and N_{SST}; relative values of the total lengths of lineaments..

before the strong seismic events on 6 February 2023 of $M = 7.5$ and $M = 7.8$. 18 days before the earthquakes, a gradual OLR decrease by $96\,\text{W/m}^2$ was revealed.

5–13 days before the foreshock that occurred on 15 January 2023 ($M = 4.7$), trends towards a decrease in temperatures and OLR were identified, while the values of LHF and RHS increased. RHS increase (by 24%) probably influenced the increase in LHF values (by $13\,\text{W/m}^2$) detected 10 days before the foreshock. 12 days before the shock, a tendency for OLR decrease (by $72\,\text{W/m}^2$) was discovered.

Analysis of changes in daily average AOD in the earthquake-affected area revealed anomalies characterized by gradual growth of values by 144% relative to the average annual value exceeding the 99% confidence interval 7–8 days before the main $M = 7.8$ seismic event, followed by a decline by 94% below the annual average value.

Similar anomalies were also observed for other earthquakes with $M = 4.0$–5.6 that occurred in the studied region in August–September 2020. The excess of the annual average AOD value was 219% and 129% for the earthquakes occurred on 4 August and 8 September 2020, respectively.

Based on the research results of ionospheric plasma parameter variations during the preparation and occurrence of a series of destructive earthquakes in Türkiye in February 2023, seismo-ionospheric anomalies were identified using GPS data. These anomalies manifested in N_e drop at the maximum height of F2 layer (by ~ 20–30%) recorded from vertical profiles on 3 February 2023 (3 days before the earthquake) and a sharp increase by 30–42% on 6 February 2023 (on the day of the devastating earthquakes).

It should be noted that pre-seismic anomalies, expressed as a drop in N_e values at the maximum height of F2 layer, recorded 1–8 days before earthquakes, as well as their sharp increase on the days of earthquakes, were obtained by us earlier, for example [*Bondur and Smirnov*, 2005; *Bondur et al.*, 2022].

Comparison of changes in thermal fields and RHS in 2023 with the background values of these parameters in 2011 verified that the detected anomalous processes were associated with the preparation of the earthquakes that occurred in Türkiye in February 2023.

The joint analysis of the results of the conducted research revealed timed sequences of anomalies in parameters of various geophysical fields (lineament systems, SST, SAT, RHS, LHF, OLR, AOD, and TEC) during the preparation of a series of destructive earthquakes in Türkiye in February 2023.

It was found that before the onset of destructive earthquakes in Türkiye on 6 February 2023 there was a general decrease in values of N_{SST} and N_{SAT} (2–18 days before), N_{OLR} (2–16 days before), NTEC (3 days before), and AOD (2–9 days before). Along with this, increased N_{RHS} values were registered (4–19 days before the destructive earthquakes), which are likely associated with a N_{LHF} increase during the same period. It was also identified that there was a decrease in the number of lineament systems in directions consistent with the extension of the main relief structures of the studied region and an increase in intersecting lineaments 3–14 days before the earthquake on 6 February 2023.

Thus, the analysis of various parameters of geophysical fields registered using satellite data showed that anomalies of all parameters studied in this work most intensely manifested themselves 3–13 days before the start of a series of earthquakes in Türkiye in February 2023.

The conducted research demonstrated that for a better understanding of the processes associated with the preparation of earthquakes, it is promising to carry out a joint analysis of the parameters of various geophysical fields registered from satellite and other data. These parameters can be used as short-term precursors of significant seismic events when monitoring seismically hazardous areas.

References

Akhoondzadeh, M. (2015), Ant Colony Optimization detects anomalous aerosol variations associated with the Chile earthquake of 27 February 2010, *Advances in Space Research*, *55*(7), 1754–1763, https://doi.org/10.1016/j.asr.2015.01.016.

Akhoondzadeh, M., and D. Marchetti (2023), Study of the Preparation Phase of Turkey's Powerful Earthquake (6 February 2023) by a Geophysical Multi-Parametric Fuzzy Inference System, *Remote Sensing*, *15*(9), 2224, https://doi.org/10.3390/rs15092224.

Bondur, V. G., and V. M. Smirnov (2005), Method for monitoring seismically hazardous territories by ionospheric variations recorded by satellite navigation systems, *Doklady Earth Sciences*, *403*(5), 736–740, EDN: LJHLVP.

Bondur, V. G., I. A. Garagash, M. B. Gokhberg, and M. V. Rodkin (2016), The evolution of the stress state in Southern California based on the geomechanical model and current seismicity, *Izvestiya*, *Physics of the Solid Earth*, *52*(1), 117–128, https://doi.org/10.1134/S1069351316010043.

Bondur, V. G., M. N. Tsidilina, E. V. Gaponova, and O. S. Voronova (2022), Combined Analysis of Anomalous Variations in Various Geophysical Fields during Preparation of the M5.6 Earthquake near Lake Baikal on September 22, 2020,

Based on Satellite Data, *Izvestiya, Atmospheric and Oceanic Physics*, 58(12), 1532–1545, https://doi.org/10.1134/S0001433822120052.

Bondur, V. G., T. N. Chimitdorzhiev, and A. V. Dmitriev (2023), Anomalous Geodynamics before the 2023 Earthquake in Turkey According to Radar Interferometry 2018-2023, *Issledovanie Zemli iz Kosmosa*, 2023(3), 3–12, https://doi.org/10.31857/S0205961423030090 (in Russian).

Cervone, G., R. P. Singh, M. Kafatos, and C. Yu (2005), Wavelet maxima curves of surface latent heat flux anomalies associated with Indian earthquakes, *Natural Hazards and Earth System Sciences*, 5(1), 87–99, https://doi.org/10.5194/nhess-5-87-2005.

Dal Zilio, L., and J.-P. Ampuero (2023), Earthquake doublet in Turkey and Syria, *Communications Earth & Environment*, 4(1), https://doi.org/10.1038/s43247-023-00747-z.

Dey, S., and R. P. Singh (2003), Surface latent heat flux as an earthquake precursor, *Natural Hazards and Earth System Sciences*, 3(6), 749–755, https://doi.org/10.5194/nhess-3-749-2003.

Federal Research Center Geophysical Survey of the RAS (2023), Catalog of the last earthquakes from 2000 to 2023, http://www.ceme.gsras.ru (in Russian), (visited on 12/08/2023).

Ganguly, N. D. (2016), Atmospheric changes observed during April 2015 Nepal earthquake, *Journal of Atmospheric and Solar-Terrestrial Physics*, 140, 16–22, https://doi.org/10.1016/j.jastp.2016.01.017.

Ghosh, S., S. Sasmal, M. Naja, S. Potirakis, and M. Hayakawa (2023), Study of aerosol anomaly associated with large earthquakes (M>6), *Advances in Space Research*, 71(1), 129–143, https://doi.org/10.1016/j.asr.2022.08.051.

Google Earth Engine (2023), MCD19A2 Level 2 data product 2000-2023, https://earthengine.google.com/, (visited on 12/20/2023).

Gvishiani, A. D., A. A. Soloviev, and B. A. Dzeboev (2020), Problem of Recognition of Strong-Earthquake-Prone Areas: a State-of-the-Art Review, *Izvestiya, Physics of the Solid Earth*, 56(1), 1–23, https://doi.org/10.1134/s1069351320010048.

Hearty, T., A. Savtchenko, M. Theobald, et al. (2013), *Readme document for AIRS version 006 products*, NASA, GES DISC.

Jiao, Z., J. Zhao, and X. Shan (2018), Pre-seismic anomalies from optical satellite observations: a review, *Natural Hazards and Earth System Sciences*, 18(4), 1013–1036, https://doi.org/10.5194/nhess-18-1013-2018.

Keilis-Borok, V., A. Gabrielov, and A. Soloviev (2009), Geo-complexity and Earthquake Prediction, in *Encyclopedia of Complexity and Systems Science*, pp. 4178–4194, Springer New York, https://doi.org/10.1007/978-0-387-30440-3_246.

Lyapustin, A., and Y. Wang (2018), MCD19A2 MODIS/Terra+Aqua Land Aerosol Optical Depth Daily L2G Global 1km SIN Grid V006, https://doi.org/10.5067/MODIS/MCD19A2.006.

Mikhailov, V. O., I. P. Babayants, M. S. Volkova, et al. (2023a), Reconstruction of Co-Seismic and Post-Seismic Processes for the February 6, 2023 Earthquake in Turkey from Data of Satellite SAR Interferometry, *Izvestiya, Physics of the Solid Earth*, 59(6), 888–898, https://doi.org/10.1134/S1069351323060113.

Mikhailov, V. O., I. P. Babayantz, M. S. Volkova, et al. (2023b), The February 6, 2023, Earthquakes in Turkey: A Model of the Rupture Surface Based on Satellite Radar Interferometry, *Doklady Earth Sciences*, 511(1), 571–577, https://doi.org/10.1134/S1028334X23600627.

Mogi, K. (1985), *Earthquake Prediction*, Academic Press, Tokyo.

Molchan, G., and V. Keilis-Borok (2008), Earthquake prediction: probabilistic aspect, *Geophysical Journal International*, 173(3), 1012–1017, https://doi.org/10.1111/j.1365-246X.2008.03785.x.

Noll, C. E. (2010), The crustal dynamics data information system: A resource to support scientific analysis using space geodesy, *Advances in Space Research*, 45(12), 1421–1440, https://doi.org/10.1016/j.asr.2010.01.018.

Okada, Y., S. Mukai, and R. P. Singh (2004), Changes in atmospheric aerosol parameters after Gujarat earthquake of January 26, 2001, *Advances in Space Research*, 33(3), 254–258, https://doi.org/10.1016/S0273-1177(03)00474-5.

Pulinets, S., and D. Ouzounov (2011), Lithosphere-Atmosphere-Ionosphere Coupling (LAIC) model - An unified concept for earthquake precursors validation, *Journal of Asian Earth Sciences*, *41*(4–5), 371–382, https://doi.org/10.1016/j.jseaes.2010.03.005.

Pulinets, S. A., D. Ouzounov, A. V. Karelin, K. A. Boyarchuk, and L. A. Pokhmelnykh (2006), The physical nature of thermal anomalies observed before strong earthquakes, *Physics and Chemistry of the Earth*, *Parts A/B/C*, *31*(4–9), 143–153, https://doi.org/10.1016/j.pce.2006.02.042.

Ruzhich, V. V., L. P. Berzhinskaya, E. A. Levina, and E. I. Ponomareva (2023), On the causes and consequences of two devastating earthquakes in the Türkiye on February 6, 2023, *Geology and Environment*, *3*, 22–34, https://doi.org/10.26516/2541-9641.2023.1.22.

Saha, S., S. Moorthi, H.-L. Pan, et al. (2010), The NCEP Climate Forecast System Reanalysis, *Bulletin of the American Meteorological Society*, *91*(8), 1015–1058, https://doi.org/10.1175/2010bams3001.1.

Smirnov, V. M., and E. V. Smirnova (2008), Investigation of the Possibility of Satellite Navigation System Application for Seismic Event Monitoring, *Electromechanics problems*, *105*, 94–104 (in Russian), EDN: KDSVGL.

Sobolev, G. A., and A. V. Ponomarev (2003), *Earthquake physics and precursors*, Nauka, Moscow (in Russian), EDN: RVEBFL.

Soloviev, A. A., and A. I. Gorshkov (2017), Modeling the dynamics of the block structure and seismicity of the Caucasus, *Izvestiya*, *Physics of the Solid Earth*, *53*(3), 321–331, https://doi.org/10.1134/S1069351317030120.

Trifonov, V. G. (2017), Neotectonics of Mobile Belts, in *Transactions of the Geological Institute*, 614, p. 180, GEOS, Moscow (in Russian), EDN: RTGVPV.

Tronin, A. A. (2000), Thermal IR satellite sensor data application for earthquake research in China, *International Journal of Remote Sensing*, *21*(16), 3169–3177, https://doi.org/10.1080/01431160050145054.

United States Geological Survey (2023), Catalog of the last earthquakes from 2000 to 2023, https://earthquake.usgs.gov, (visited on 12/08/2023).

World Data System (2023), World Data Center for Geomagnetism, Kyoto, http://wdc.kugi.kyoto-u.ac.jp/index.html, (visited on 11/20/2023).

Xiong, P., X. H. Shen, Y. X. Bi, et al. (2010), Study of outgoing longwave radiation anomalies associated with Haiti earthquake, *Natural Hazards and Earth System Sciences*, *10*(10), 2169–2178, https://doi.org/10.5194/nhess-10-2169-2010.

Xu, Y., T. Li, X. Tang, X. Zhang, H. Fan, and Y. Wang (2022), Research on the Applicability of DInSAR, Stacking-InSAR and SBAS-InSAR for Mining Region Subsidence Detection in the Datong Coalfield, *Remote Sensing*, *14*(14), 3314, https://doi.org/10.3390/rs14143314.

Zhang, L., K. Dai, J. Deng, et al. (2021), Identifying potential landslides by stacking-insar in southwestern china and its performance comparison with sbas-insar, *Remote Sensing*, *13*(18), 3662, https://doi.org/10.3390/rs13183662.